DOI: 10.1590/2317-4889201820170124

ARTICLE

Gold deposits in poly-deformed metasedimentary rocks: a case study of the C1-Santaluz gold deposit, Itapicuru Greenstone Belt, Northeast of Brazil

José Antonio Cirillo de Assis[1]*, George Luiz Luvizotto[1]

ABSTRACT: *The C1-Santaluz gold deposit is located in the Itapicuru greenstone belt in Bahia State, Brazil. Metavolcanic and metasedimentary rocks dominate at the base and top, respectively. The ore minerals related to the auriferous mineralization are pyrite, arsenopyrite, sphalerite, chalcopyrite and stibnite. Arsenopyrite is related to, and associated with the presence of gold in quartz veins, a feature which is detected by scanning electron microscope analyses. The deposit is structurally complex, with tree deformational phases being recognized: D_{n-1}, D_n, and D_{n+1}. Phases D_{n-1} and D_n have a direct relation to the mineralization, and mineralized quartz veins are parallel to the S_n foliation ($S_0//S_{n-1}//S_n$). The intersection between the $S_0//S_{n-1}$ bedding and the S_n foliation generates an intersection lineation parallel to the D_n fold axis, plunging to the NW, which has favored an increase in the volume of mineralized bodies.*

KEYWORDS: *Structural settings; auriferous mineralization; sulfide assemblage.*

INTRODUCTION

Structural controls play a major role in gold deposits, and understanding the different structures and their relationships with one another is fundamental to the interpretation of the gold system.

According to Groves *et al.* (2003), there are important factors regarding orogenic gold deposits (definition after Groves *et al.* 1998), such as the source of ore fluids and metals, tectonic setting, age of mineralization of some provinces, features of hydrothermal alteration and depositional mechanisms specific to gold. These factors are not always well known during the exploration phase and may be compared to those from important world-class deposits already documented, leading to a better understanding of their characteristics. Assessing the structural factors that contribute to gold deposition can aid gold exploration.

The genesis of most orogenic gold deposits around the world is closely related to the processes of metamorphism and deformation, with orebodies commonly formed in low metamorphic grade (Large *et al.* 2011). The main orogenic gold deposits are strongly associated with deformed metamorphic terranes, and gold is commonly related to greenschist facies rocks (Groves *et al.* 1998, 2000, 2003, Hagemann & Cassidy 2000, Goldfarb *et al.* 2005, Goldfarb & Groves, 2015).

The Rio Itapicuru greenstone belt (RIGB) is an important geological entity located at the northeastern region of Brazil, in Bahia State, and hosts two main auriferous deposits, Fazenda Brasileiro and C1-Santaluz (Fig. 1).

The Fazenda Brasileiro gold deposit is located in the meridional part of the RIGB, and has been the subject of several studies (Kishida 1979, Marimom *et al.* 1986, Xavier 1987, Reinhardt 1988, Reinhardt & Davison 1989, Teixeira *et al.* 1990, Mello *et al.* 1996, Alves da Silva *et al.* 1998, Vieira *et al.* 1998, Silva *et al.* 2001, Pimentel & Silva 2003). The C1-Santaluz deposit is located in the central portion of the belt (Fig. 1) and is the focus of the present study.

[1]Instituto de Geociências e Ciências Exatas, Universidade Estadual Paulista "Júlio de Mesquita Filho" – São Paulo (SP), Brazil. *E-mails: jcirillo.assis@gmail.com, georgell@rc.unesp.br*

*Corresponding author

Manuscript ID: 20170124. **Received on:** 09/23/2016. **Approved on:** 08/27/2018.

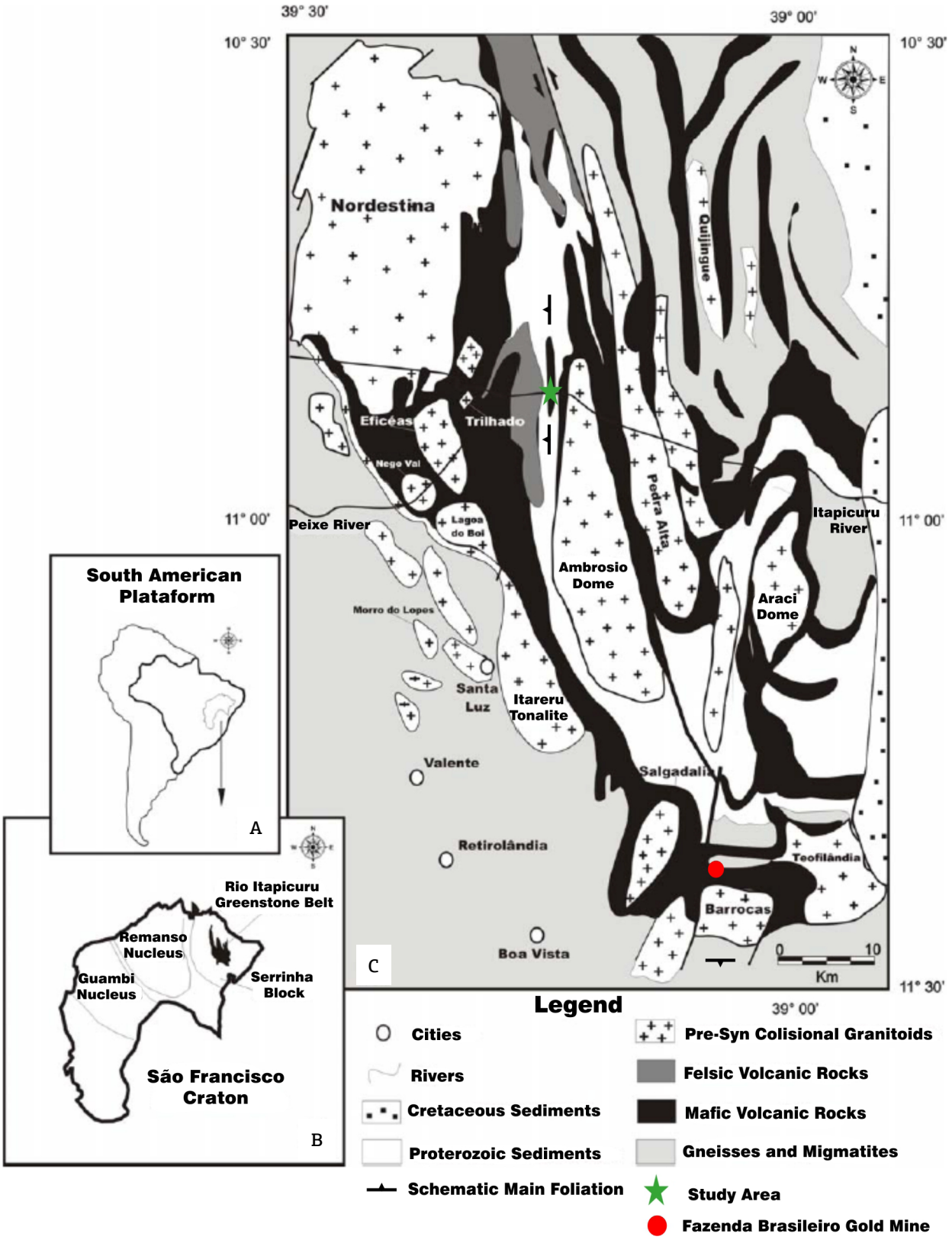

Figure 1. (A) São Francisco Craton highlighted in the South American Plataform. (B) The basement terrains of the São Francisco Craton, as well as the Rio Itapicuru greenstone belt located in the Serrinha Block. (C) Geological map of the Rio Itapicuru greenstone belt. The green star represents the current study area, the C1-Santaluz deposit. Modified from Donatti Filho (2007).

As a structurally controlled gold deposit, C1-Santaluz (Fig. 2) has features that correspond to an orogenic auriferous mineralization, similar to those described by Colvine *et al.* (1984), Robert (1996), Goldfarb *et al.* (2001), such as poly-deformed host rocks, greenschist facies assemblage (sulfide-carbonate-chlorite-sericite), low sulfide volume and strong degree of structural control.

The RIGB auriferous mineralization results from hydrothermal fluid influx in magnetite and carbonaceous schists, carbonate-quartz veins, gabbros and breccias (see, for example, Kishida 1979). Ruggiero (2008) points out the presence of gold in the RIGB in association with small- to medium-scale shear zones, typical of orogenic lode gold deposits. Vasconcelos and Becker (1992) and Mello *et al.* (2006) constrained the age of the Fazenda Brasileiro mineralization to 2.083–2.031 Ga.

Fazenda Brasileiro deposit mineralization was formed under temperature conditions of 250–400ºC, and the orebodies were developed primarily as stratabound with free gold in quartz veins emerging at a later stage (Teixeira 1984). Reinhardt (1988) points out that gold also occurs as ore shoots (rods) marked by quartz veins orientated along the stretching lineation parallel to an intersection lineation. Furthermore, breccia zones tend to be enriched in gold with metal grades strictly related to the presence of arsenopyrite and pyrite.

The C1-Santaluz gold deposit is hydrothermally associated with shear zones and folds, in a poly-deformed scenario.

Geochronological Ages

Bloco Gavião	TTG's granites	3.4-3.2 Ga	U-Pb SHRIMP	Marinho (1991)
Bloco Gavião	greenstone belts	3.3, 3.2, 3.0-2.8 Ga	U-Pb SHRIMP	Marinho (1991)
RIGB	granitic intrusions	3.0-2.9 Ga	zircon U-Pb	Gaál et al. (1987)
Rio Capim greenstone b.		2.22-2.09 Ga	whole-rock Pb-Pb; zircon U-Pb	Oliveira et al. (1998)
RIGB	mafic volcanic unit	2.2 Ga	whole-rock Pb-Pb; whole-rock Sm-Nd	Silva (1992)
RIGB	Trilhado granodiorite	2.1 Ga	monazite U-Pb SHRIMP	Mello et al. (2006)
RIGB	Nordestina granodiorite	2.1 Ga	zircon U-Pb SHRIMP	Cruz Filho et al. (2005), Donatti Filho et al. (2013)
RIGB	Barrocas granodiorite	2.1 Ga	zircon Pb evaporation	Chauvet et al. (1997)
RIGB	Itareru tonalite	2.1 Ga	zircon U-Pb SHRIMP	Carvalho and Oliveira (2003)
RIGB	tholeiitic basalts	2.1 Ga	zircon U-Pb SHRIMP	Oliveira et al. (2010)
RIGB	felsic volcanic unit	2.1-2.08 Ga	whole-rock Pb-Pb	Silva et al. (2001)
RIGB	Pedra Vermelha granite	2.08 Ga	isotope-dilution zircon U-Pb	Rios et al. (2005)
RIGB	Ambrósio granodiorite	2.08 Ga	xenotime U-Pb SHRIMP	Mello et al. (2006)
RIGB	auriferous mineralization	2.08-2.03 Ga	muscovite Ar-Ar	Vasconcelos and Becker (1992), Mello et al. (2006)
RIGB	Morro dos Lopes granite	2.07 Ga	isotope-dilution zircon U-Pb	Rios et al. (2000)
RIGB	kimberlitic intrusions	0.64 Ga	peroviskite U-Pb	Donatti Filho et al. (2012)

RIBG: Rio Itapicuru greenstone belt.

Figure 2. Synthesis of the geochronological ages of the RIGB and its surrounding lithotypes.

Therefore, understanding the structural framework of the study area is a key task because it can help guide future prospective work, not only in the study area but in other structurally complex localities.

The main goal of this paper is to characterize the structural evolution of the C1-Santaluz deposit. To attain this objective, geological and structural mapping of the area was undertaken, including description and interpretation of deformational features, both at macro- and microscopic scales. The paper also discusses stratigraphic and petrographic features, as well as types of gold occurrences, including the sulfide minerals present in quartz and carbonate-quartz veins. Mineralogical studies are aided by analytical XRD, SEM and BSE data.

REGIONAL GEOLOGICAL SETTING

São Francisco Craton (Fig. 1) is located in northeast central Brazil (Almeida 1977, Alkmim 2004). Together with the African plate, São Francisco Craton forms San Francisco-Congo Craton (Almeida *et al.* 1976; Alkmim 2004), which was part of the western Gondwana prior to the formation of the Atlantic Ocean in the Cretaceous. At the end of the Neoproterozoic, this supercontinent comprised a group of tectonic plates that were coalesced by successive diachronic collisions (Alkmim 2004). According to Almeida (1977) and Almeida *et al.* (1981), São Francisco Craton is bordered by Neoproterozoic belts, and northern exposures preserve features of Paleoproterozoic orogens, divided into four main lithotectonic compartments, namely, Gavião, Serrinha, Jequié Blocks, and the Itabuna-Salvador-Curaçá Belt (Barbosa & Sabaté 2002, 2004).

Serrinha Block is located in the northeastern portion of the Craton and forms an oval structure of approximately 21,000 km^2. It is composed of migmatized orthogneisses superposed by sequences of greenschist-facies supracrustal rocks intruded by granites (Gaál *et al.* 1987, Alves da Silva 1994). The RIGB belongs to Serrinha Block, and is 100-km long (N-S) and 30-km wide (E-W) (Chauvet *et al.* 1997, Alves da Silva 1998). It is a metavolcano-sedimentary sequence intruded by syn- to post-tectonic granites (Silva 1992).

The supracrustal rocks of the RIGB are approximately 9.5-km wide covering an area of 7,500 km^2 and are composed of mafic volcanic rocks, at the base, and felsic/intermediate volcanic and metasedimentary rocks at the top (Kishida 1979, Kishida & Riccio 1980, Silva 1992). The whole sequence is characterized by low-grade metamorphism (Kishida 1979).

They have a preferred N-S orientation in the central and northern parts, where geological contacts are typically parallel to the main foliation. In the southern part, the preferred orientation is E-W (Silva 1992) (Fig. 1).

According to Kishida (1979) and Silva (1992), the RIGB supracrustal rocks are Paleoproterozoic and may reach up to 9.5 km in thickness. From bottom to top, they are divided into three domains and intrusive rocks are commonly present (Kishida 1979; Silva 1983; Silva et al. 2001, Barbosa and Sabaté 2004):

1. a volcanic mafic unit, composed of metamorphosed tholeiitic basalts and mafic tuffs with associated iron formations, cherts and graphitic phyllites;
2. a volcanic intermediate to felsic unit, consisting of felsic rocks of andesitic to dacitic, calc-alkaline composition, with aphanitic, porphyritic, variolitic and pyroclastic texture, also exemplified by tuff and agglomerate lapillis;
3. a sedimentary unit, characterized by conglomerates, phyllites, sandstones and siltstones, which may be associated with banded iron formations, marbles, gondites and cherts.

The basal volcanic mafic unit is aged 2,209 ± 60 Ma (Pb-Pb whole rock method) and a Sm-Nd TDM age (whole-rock) of 2.2 Ga (Silva 1992, Barbosa & Sabaté 2004). Oliveira *et al.* (2010) presented U-Pb SHRIMP ages in zircons of 2,145 ± 8 Ma and 2,142 ± 6 Ma for tholeiitic basalts of the sequence.

Silva (1992) presented ages of 2,080 ± 90 Ma (Rb-Sr), 2,109 ± 80 Ma (Pb-Pb) and 2.1 Ga (Sm-Nd) for the volcanic intermediate to felsic unit. Grisólia (2010) also states that the metasedimentary rocks (in the sedimentary unit) of the RIGB are Paleoproterozoic, with deposition ages between 2,110–2,120 Ma for Sm-Nd isotopes. Grisólia (2010) also adds that these rocks originated either from the erosion of the RIGB itself, or from other sources with similar ages.

Several intrusive bodies (dikes and sills) occur in the RIGB and are represented by diorite and gabbro of tholeiitic composition (Kishida 1979, Silva 1992). Granitic bodies have ellipsoidal shapes and may be grouped into two main types: granite-gneiss domes, and isotropic bodies that intrude the supracrustal sequence (Kishida 1979; Rocha Neto 1994). According to Silva (1992), these bodies may be syn- or post-tectonic, and are related to the first deformation phase of the structural setting.

Syn-tectonic granitic intrusions are associated with the drift phase of the Rio Itapicuru volcano-sedimentary basin and are represented by granitoids such as Barrocas, Teofilândia and Nordestina (Fig. 1), which have a calcium-alkaline nature and Paleoproteozoic ages (Rios *et al.* 2003). Post-tectonic granitoids intruding into the RIGB rocks are alkaline and represented by Ambrósio and Pedra Vermelha (Rios *et al.* 2003). They have an U-Pb SHRIMP (xenotime) age of 2,080 ± 2 Ma (Mello *et al.* 2006) and an U-Pb isotope dilution (zircon) age of 2,080 ± 8 Ma (Rios *et al.* 2005),

respectively. A summary of ages presented in the literature is shown in Figure 2.

Kishida (1979) and Silva (1992) indicate that ultramafic bodies are composed of carbonate-rich, serpentinized peridotites. They have an elongated shape, which is displayed parallel to the regional foliation. Kimberlite intrusions are also documented in the RIGB. The main body occurs at the Nordestina batholith, as an elongated intrusion with a N30W direction with an age (U-Pb perovskite) of 642 ± 6 Ma (Donatti Filho *et al.* 2012).

Silva (1992) proposes a back-arc basin type evolutive model for the RIGB. Kishida (1979) interprets the RIGB metasedimentary rocks from the top of the sequence as volcanoclastic.

Gold mineralization at the C1-Santaluz deposit

C1-Santaluz is the main gold deposit in the central part of the RIGB, presently being mined. Formerly known as Fazenda Maria Preta, the mine was explored by Vale S.A. (former Companhia Vale do Rio Doce) from the early 1980's until the 1990's, when it was passed on to Companhia Baiana de Pesquisa Mineral (CBPM). It was later decommissioned, and, in 2003, Yamana Gold Inc. bought the property and started an exploration program, which continued after mining began in 2008. In 2013, the mine was decommissioned due to operational problems. In 2015, Brio Gold Inc., the subsidiary of Yamana Gold Inc., was created and became the exploration and mining group at the C1-Santaluz deposit.

The extraction ranges from low- to -high gold grades, with proven and probable mineral reserves of 1.2 million ounces of gold, which corresponds to 26.7 million tonnes at 1.42 g/t (at the end of 2016). It also has measured and indicated resources of 780,000 ounces at 1.95 g/t Au, as well as 395,000 ounces at 2.07 g/t Au of inferred resources. The forecast scenario is for an annual production of 114,000 ounces of gold (after decommission, in 2018), with a recovery rate of 84% (Brio Gold Inc., 2017).

Mineralization in C1-Santaluz is hosted at the contact between an intrusive body of intermediate composition and brecciated metasedimentary rocks, with veins, quartz veinlets, and quartz-veined stockwork zones, typically with sulfide minerals. The auriferous mineralization in quartz and quartz-carbonate veins is associated with ductile N-S shear zones, all hosted in a carbonaceous phyllite (Xavier 1987, Carvalho 1991).

The mineralized veins have a N40E preferred orientation; according to Alves da Silva *et al.* (1998), veins are embedded in a ductile-brittle shear zone that follows the main contact between the ore and the hanging wall. At depth, quartz veins occur in brecciated carbonaceous phyllite, and are typically associated with lenses of brecciated metadacite. These lenses may be mineralized and correspond to 10% of the ore deposit (Alves da Silva *et al.* 1998). Coelho and Silva (1998) describe hydrothermal alteration dominated by silicification, and enrichment of pyrite and albite related to the auriferous C1-Santaluz deposit, normally appearing in quartzose stockwork structures.

METHODS

This work was carried out based on field work, sample descriptions, drill core logging, as well as laboratory analyses, such as petrographic, microstructural, scanning electron microscope and X-ray diffraction analyses with the purpose of better describing the geology of the C1-Santaluz deposit.

A detailed map of the C1-Santaluz deposit is presented (Fig. 3) with the support of descriptions by the Yamana Gold Inc.'s drill holes, and results from the work by Assis (2016). A total of 34 thin sections were described identifying minerals and microstructures. Four samples were analyzed by Scanning Electron Microscopy (SEM) at the Department of Petrology and Metalogeny, State University of São Paulo. Analyses were carried out on a JOEL JSM6010LA instrument, equipped with backscattered (BSE), secondary electrons and Energy Dispersive Spectroscopy (EDS) detectors. Selected samples correspond to mineralized schists from the C1-Santaluz deposit. Analyses were performed to identify possible accessory minerals and gold occurrences in the study area.

X-Ray Diffraction (XRD) analyses were conducted at the Department of Petrology and Metallogeny, State University of São Paulo, using the PANalytical EMPYREAN diffractometer with radiation CuKα1 (WL = 1 54056 Å) and Ni filter. Analyses were carried out on four samples with carbonaceous material, not identifiable under the petrographic microscope. These rocks were classified by the author as carbonaceous phyllite and breccia. Analyses were carried out to identify the chemical structure of the carbonaceous materials.

RESULTS

Lithostratigraphic domains

Only the volcanic and metasedimentary domains, and the intermediate intrusive lithotypes are recognized in the study area. From the base to the top, and for the purpose of the present study, these have been divided into:

1. chlorite-sericite-quartz schist (metasedimentary rocks domain);
2. carbonaceous phyllite (metasedimentary rocks domain);

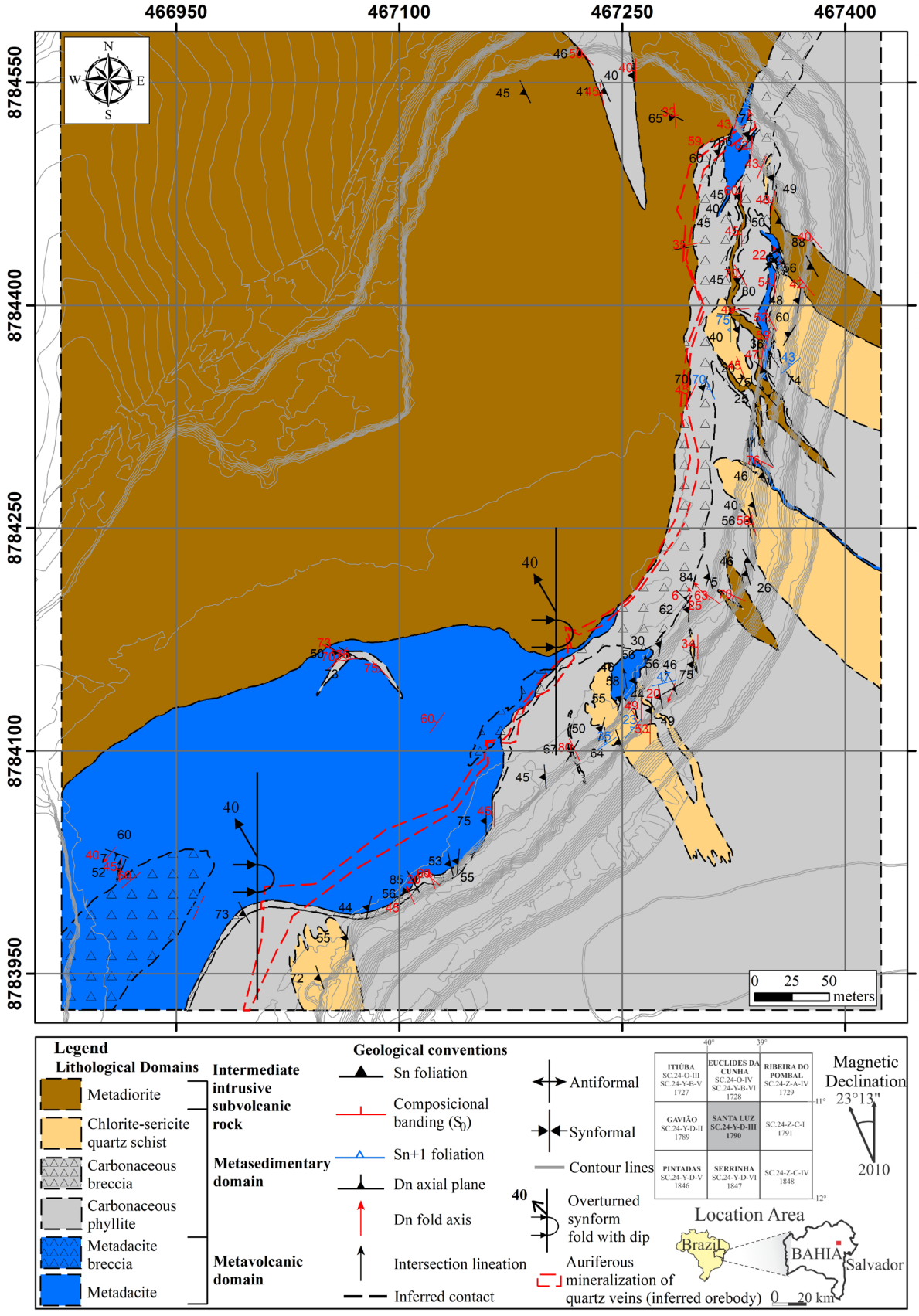

Figure 3. Geological map of the C1-Santaluz deposit, Rio Itapicuru greenstone belt (universal transverse mercator; datum: SAD 1969_UTM zone 24S).

3. carbonaceous breccia (metasedimentary rocks domain);
4. metandesite (metavolcanic rocks domain);
5. metadacite (metavolcanic rocks domain);
6. metadiorite (metamorphic intermediate intrusive rocks); and
7. quartz veins and veinlets (auriferous mineralization of quartz veins, inferred orebody in Fig. 3).

The metandesite is only observed in drill holes of Yamana Gold, and is not exposed in the study area. A schematic, simplified lithotectonic column of the C1-Santaluz deposit is shown in Figure 4.

Metavolcanic Rocks Domain

The metavolcanic rocks domain occurs at the central-eastern to eastern part of the study area (Fig. 3). It is represented by metadacite lenses striking N-S- to NE-SW (Fig. 5).

At the southern part of the C1-Santaluz deposit, the metadacite is mineralized with gold and normally embedded within metasubvolcanic and metasedimentary rocks.

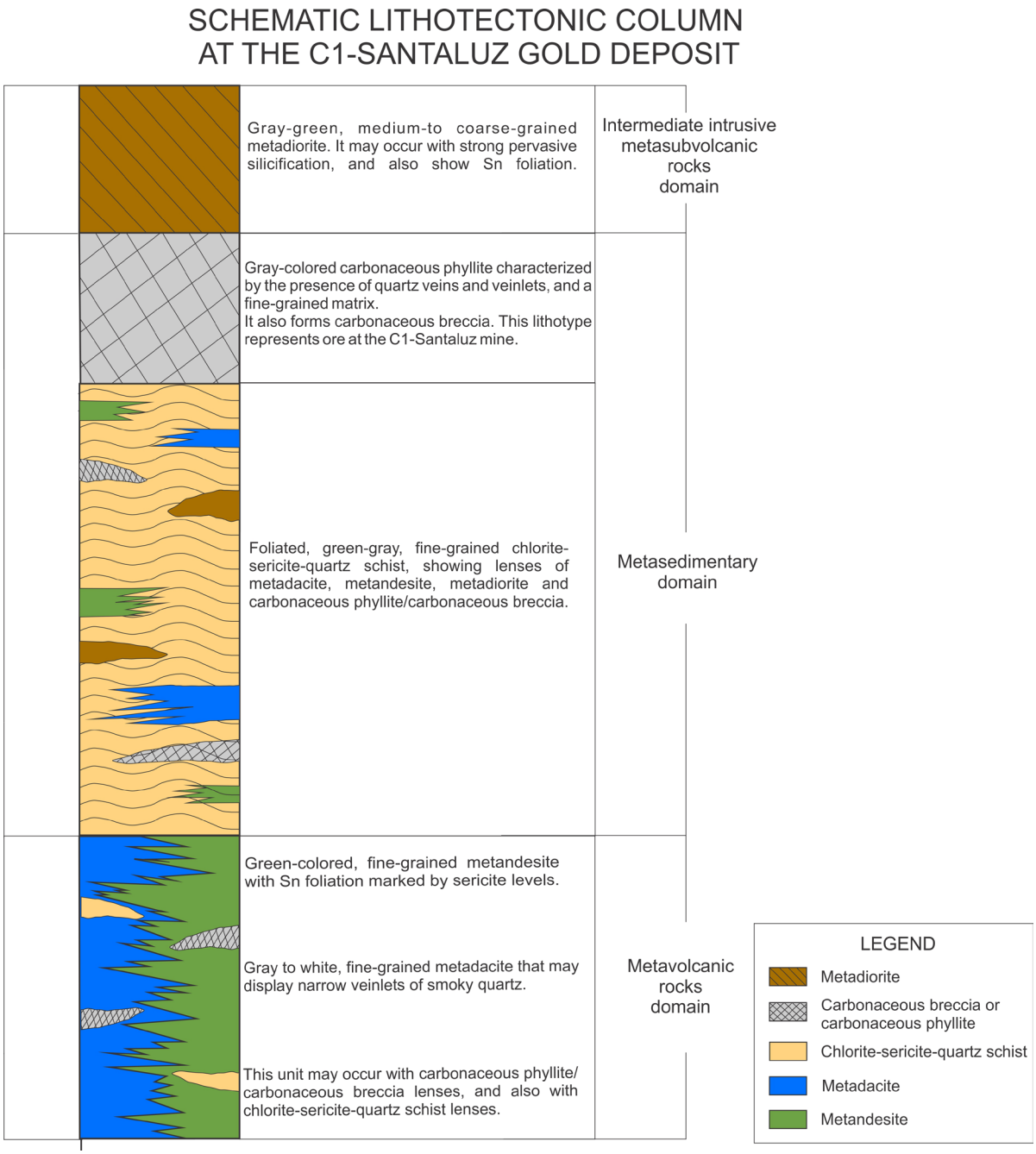

Figure 4. Schematic, proposed lithotectonic column for the C1-Santaluz gold deposit, based on Assis (2016).

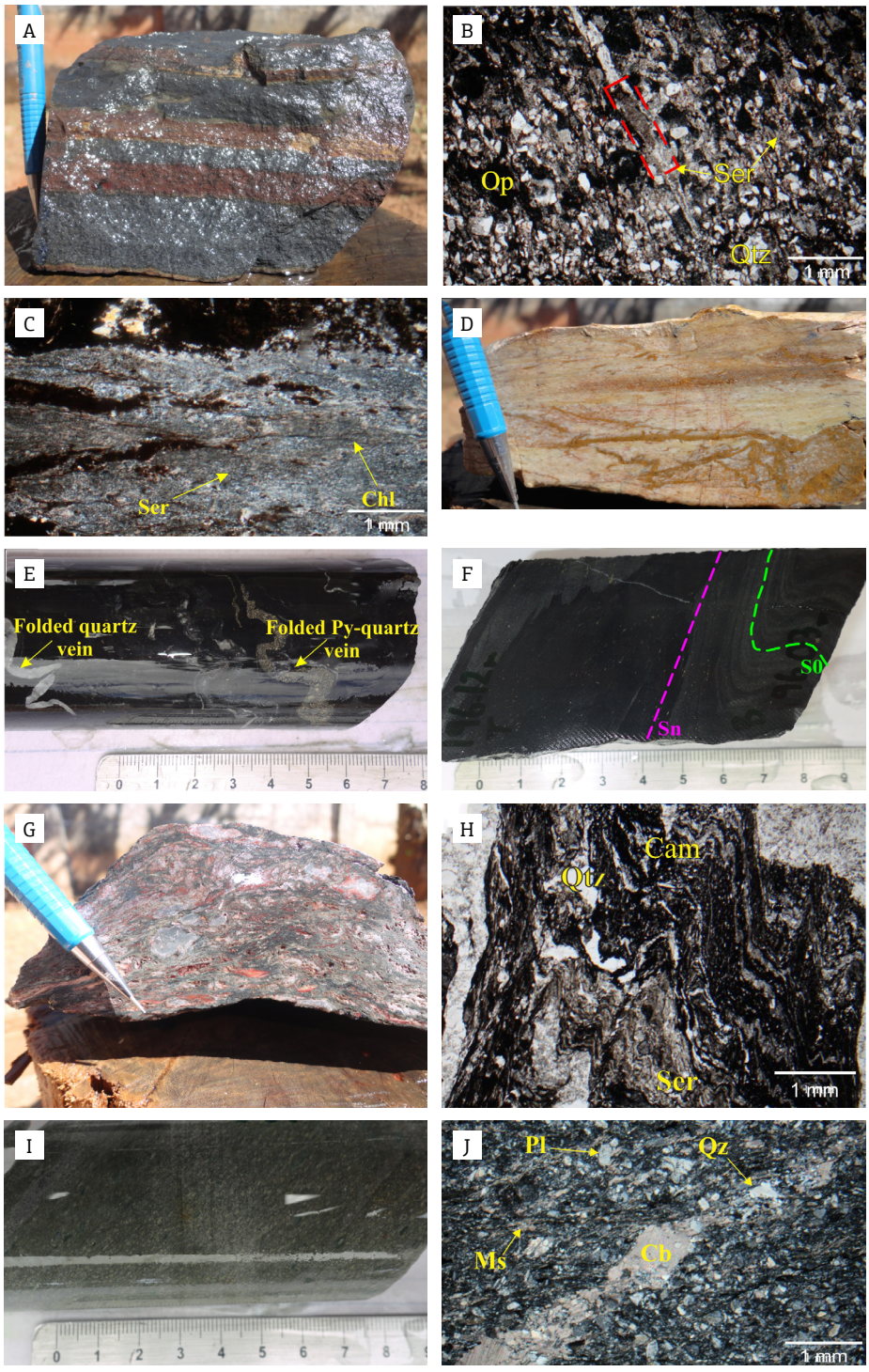

Op: opaque mineral; Ser: sericite; Qtz: quartz; Chl: chlorite; Cam: carbonaceous material; Pl: plagioclase; Ms: muscovite; Cb: carbonate mineral; Py: pyrite.

Figure 5. Macroscopic samples (A, D, E, F, G, I) and photomicrographs (B, C, H, J) of the C1-Santaluz units. (A) Gray-colored, fine-grained metadacite with oxidized bands; (B) Representative example of metadacite. Notice igneous phases transformed into sericite (highlighted by dashed, red rectangle); (C) Matrix of the chlorite-sericite-quartz schist of the Metasedimentary Domain; (D) Chlorite-sericite-quartz schist with oxidized levels; (E) Drill core sample of carbonaceous phyllite showing folded quartz and pyrite veinlets; (F) Carbonaceous phyllite collected from a drill hole showing the main foliation (S_n) parallel to the banding (S_0), with both structures folded; (G) Carbonaceous breccia with quartz veinlets, clasts and oxidized features; (H) Carbonaceous breccia showing ductile-brittle features in the matrix; (I) Drill hole of green-gray-colored metadiorite; (J) Photomicrograph showing a metadiorite containing muscovite, plagioclase, quartz, and a carbonate-quartz vein. (B, C, H and J) Cross-polarized, transmitted light photomicrographs of thin sections.

In the surrounding area, metandesite bodies are recognized, typically containing feldspar phenocrysts.

Metasedimentary Domain

The metasedimentary domain consists of chlorite-sericite-quartz schist, carbonaceous phyllite and carbonaceous breccia (Fig. 5). Rocks of this domain have a well marked foliation that is commonly folded. Outcrops are highly weathered.

The chlorite-sericite-quartz schist crops out in the central-western portion of the study area, with thicknesses varying from 10 to 120 m. The carbonaceous phyllite is up to 80 m thick, however where inserted in the domains of metadiorite and metadacite it may occur as lenticular bodies up to 20 m in thickness.

The carbonaceous phyllite sits below the metadiorite body, and has an intrusive contact relationship with this metasubvolcanic domain. A breccia with abundant quartz veinlets is situated between these two domains. In the present work, the breccia layer is classified as a separate unit, named carbonaceous breccia, as it hosts gold mineralization of the studied deposit. It occurs in the central part of the study area (Fig. 3) where it is in contact with the metadiorite; in the southern part, it is in contact with the metadacite. It has a thickness of up to 20 m and covers about 10% of the study area. In some portions, both at the macro- and microscopic scales, the matrix still preserves the main foliation and has the same preferential orientation as the carbonaceous phyllite schistosity.

Mineralized Quartz Veins of the Metasedimentary Domain

Mineralized quartz veins are contained in the carbonaceous breccia. Quartz in veins is typically white, milky to translucent. Veins are up to 60 cm thick, generally oriented parallel to the top of the metadiorite contact, and to the main foliation of the host rock. Discordant veins are also common, but are typically thinner. They are mainly perpendicular to concordant veins, and generally fill fractures (Fig. 6). Quartz veins and veinlets are associated with carbonate (ankerite identified in the SEM analysis), albite, and sulfide minerals, represented by fine-grained anhedral-euhedral aggregates of pyrite, and fine-grained anhedral-subhedral grains of arsenopyrite. Under the EDS/SEM, chalcopyrite, sphalerite and stibnite are identified in quartz veins. These opaque minerals are directly related to the auriferous mineralization at the C1-Santaluz deposit, characterizing its hydrothermal alteration.

Mineralogical data

SEM / EDS analyses

The SEM analyses were carried out to identify accessory minerals and investigate textural relationships. The study emphasizes opaque minerals since gold mineralization in the C1-Santaluz deposit is directly related to hydrothermal alteration richly represented by sulfide minerals. The lithological units analyzed are carbonaceous phyllite and breccia, and also quartz veins hosted in carbonaceous breccia.

The present sulfide minerals are pyrite, arsenopyrite and subordinate chalcopyrite, sphalerite and stibnite (Fig. 7). In addition, back scattered electron images (Fig. 8) show gold inclusion in arsenopyrite.

Also, the data indicate that, in general, the matrix of the carbonaceous phyllite and breccia is composed of sericite/muscovite, quartz, chlorite and carbonaceous material (Fig. 9).

X-Ray Diffraction Analyses (XRD)

Analyses by XRD were carried out in samples of carbonaceous phyllites and breccias. Out of the four samples analyzed, three contain amorphous carbonaceous material and one shows the presence of graphite (Fig. 9). The graphite-bearing sample is located to the east of the mineralized body at the C1-Santaluz deposit, far from the shear zone in the central part of the study area.

Metasubvolcanic Intrusive Rocks Domain

In the C1-Santaluz deposit, the metasubvolcanic bodies are always in contact with gold mineralization. Exceptions are lenses and apophyses of metadiorite, which occur in the northeastern part of the area (Fig. 3). The basal contact of these bodies with the carbonaceous breccia, as shown in Figure 3, is where the mineralized zone of the pit is located (auriferous mineralization of quartz veins).

Metadiorite is abundant in the C1-Santaluz deposit, covering about 35% of the study area. The innermost portion of the green-gray, massive metadiorite body has a granular to incipient schistose texture, and is coarse to medium grained (Fig. 5). A well marked foliation may be present at its contact with other domains. The basal contact with the carbonaceous breccia usually features sheared and/or fractured textures. The main foliation is strong in the contact zone, and has high dip angles. However, in some places, this contact truncates the main foliation of the host rock.

The metadiorite covers the western, northwestern portion of the area and has a thickness of up to 350 m (Fig. 3). In the eastern part of the area it forms lenses or apophyses of up to 20 m thick, commonly with a N-S or NW-SE strike.

Structural geology

Considering the geometric aspects and superposition criteria, the analysis of tectonic structures indicates the presence of three deformational phases, classified as D_{n-1}, D_n, and D_{n+1}. The main structure in the area is the S_n foliation,

an axial planar foliation of D_n folds that fold the compositional banding S_0. The D_n folds have axis plunging to the NW. In the metasedimentary domain, S_0 is marked by alternating layers with bands composed of quartz and sericite and bands composed of carbonaceous material. In some cases, such as in microliths of the S_n crenulation cleavage, a foliation parallel to S_0 is noted; this has been interpreted as S_{n-1}, which pre-dates S_n, from the D_{n-1} deformational phase.

The D_{n+1} phase is characterized by the folding of the S_n foliation and older structures, locally generating an axial planar foliation with a NW-SE orientation. Only the S_n foliation and structures associated with subsequent phases are present in the metasubvolcanic bodies. The metavolcanic domain shows structural features of the D_{n-1}, D_n and D_{n+1} phases. Likewise, the metasedimentary domain has structures that belong to deformation phases D_{n-1}, D_n, and D_{n+1}.

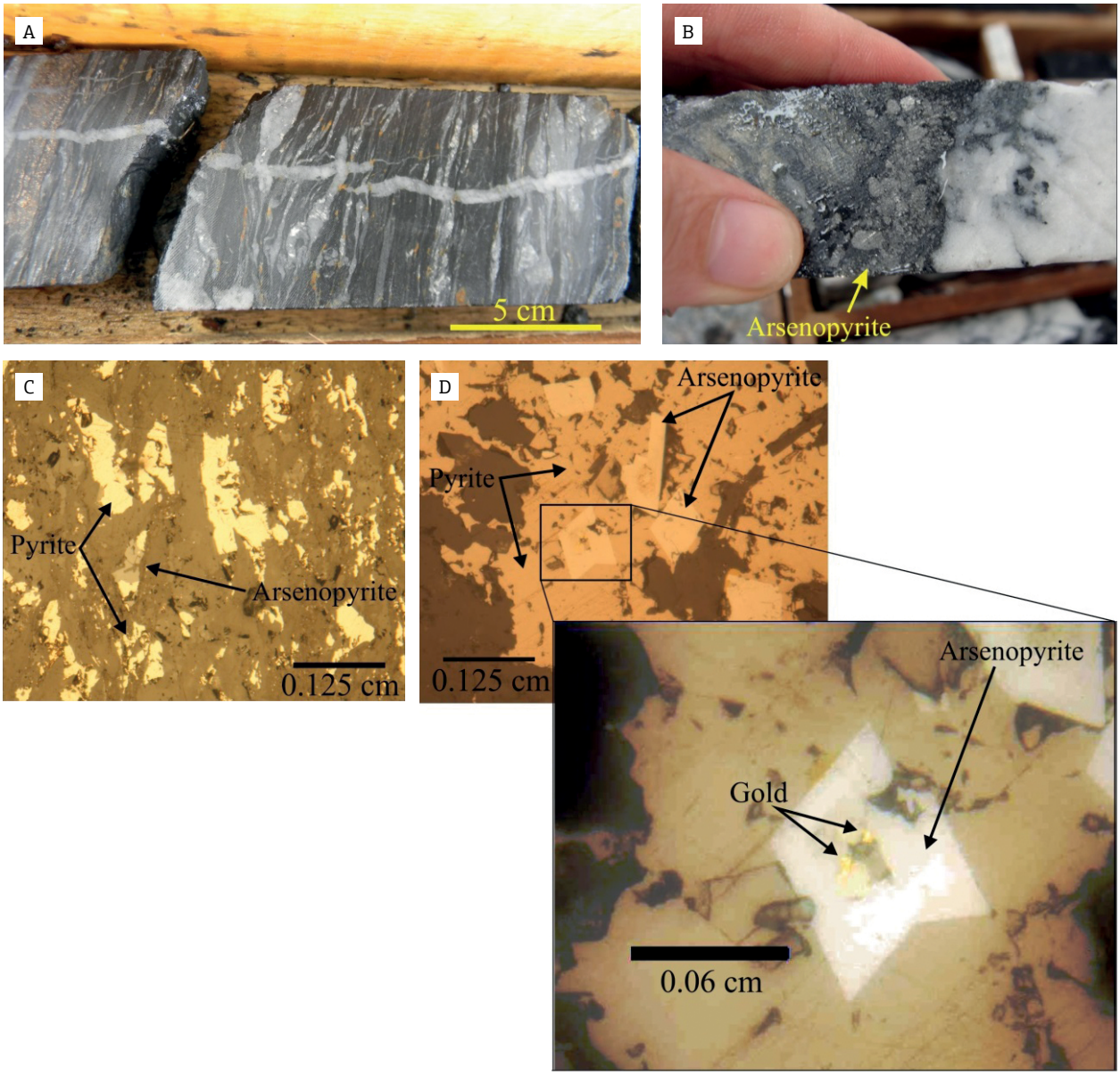

Figure 6. Drill hole samples (A, B) and photomicrographs (C, D) of quartz veins and veinlets from mineralized zones of the C1-Santaluz deposit. (A) Concordant (in respect to the main foliation) and discordant quartz veins in hydrothermally altered or silicified carbonaceous phyllite; (B) Silicified carbonaceous breccia with a quartz vein containing arsenopyrite; (C) Sulfide paragenesis represented by pyrite and arsenopyrite in hydrothermally altered carbonaceous phyllite; (D) Free gold grains in quartz vein associated with arsenopyrite in carbonaceous breccia. (C and D) Cross-polarized, reflected light, photomicrographs of thin sections.

D_{n-1} Deformation Phase

The D_{n-1} phase is marked by a foliation (schistosity) that is parallel to the rocks compositional banding S_0. It is better observed in the hinge zones of the D_n folds, where this primary structure has not been transposed by the penetrative schistosity of the D_n phase. Also, the D_{n-1} deformational phase is marked by abundant sericite in the rock matrix, which is present in phases D_n and D_{n+1}.

In the eastern part of the study area, the metasedimentary domain has a NW-SE strike, differing from the north, central and southeastern parts, where it is oriented N-S (Fig. 10). The mineralized metadiorite/carbonaceous breccia contact also has a N-S strike in the northern and southern areas, while in the central of the open pit it is oriented E-W.

Where the lithological contacts have a NW-SE strike in the east, they show an almost perpendicular relationship (truncation) with the metadiorite/carbonaceous breccia contact. In the eastern portion, the chlorite-sericite-quartz schist unit appears as a repeated layer (Fig. 10).

D_n Deformation Phase

The D_n deformation is the main evident phase in the study area. It is mainly defined by a S_n foliation, represented

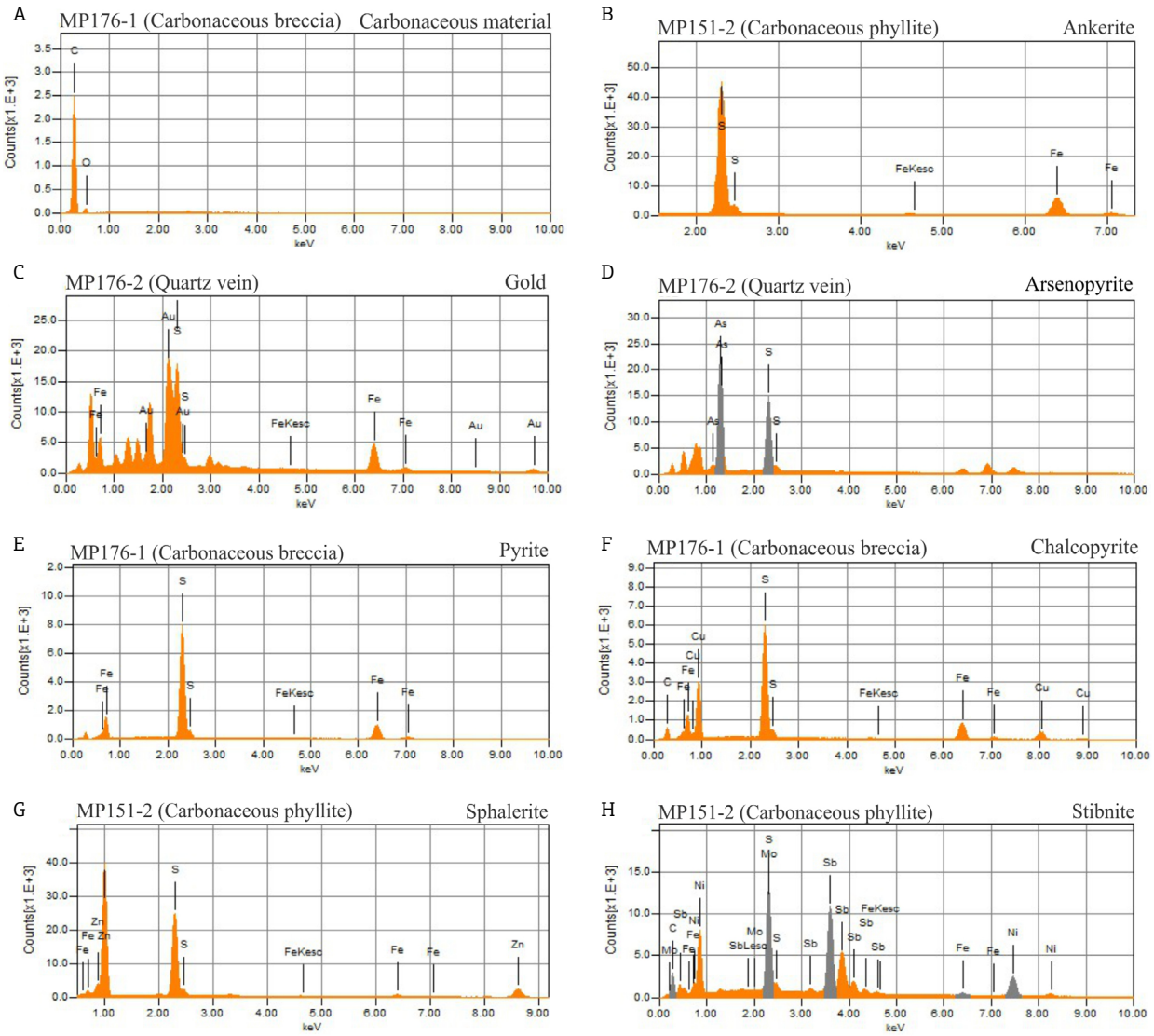

Figure 7. Intensity vs energy graphs (EDS) from the C1-Santaluz deposit obtained of: (A) Carbonaceous material present in carbonaceous breccia; (B) Ankerite in quartz veins present in carbonaceous phyllite; (C) Gold grain free in a quartz vein hosted in carbonaceous breccia; (D) Arsenopyrite in gold-bearing quartz vein of graph C; (E) Pyrite grain identified in carbonaceous breccia; (F) Chalcopyrite associated with pyrite in carbonaceous breccia; (G) Sphalerite, which represents a subordinate phase in carbonaceous phyllite; (H) Stibnite in carbonaceous phyllite, also a subordinate phase and described for the first time in the deposit.

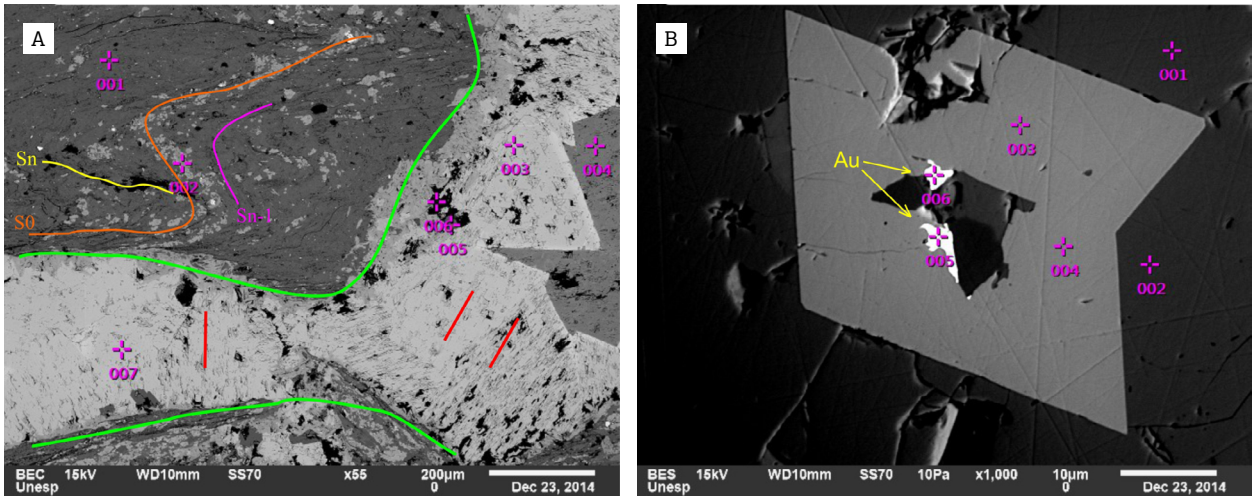

Figure 8. Scanning electron microscope (SEM) images obtained from thin sections of the C1-Santaluz deposit. (A) Carbonaceous breccia with S_0 bedding parallel to an S_{n-1} foliation, folded with planar-axial S_n foliation; (B) Free gold grains (analyses 5 and 6) associated with arsenopyrite (analyses 3 and 4) in carbonaceous breccia.

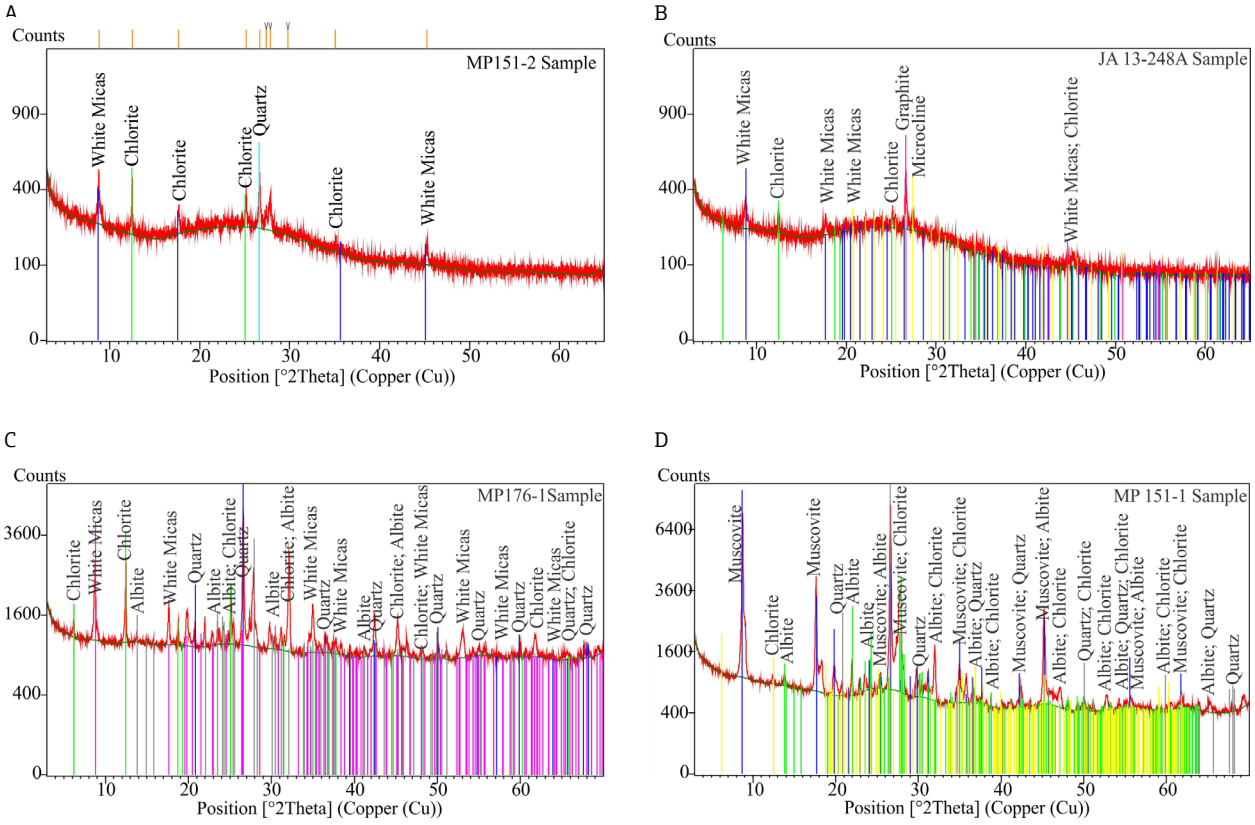

XRD: X-ray diffraction.

Figure 9. XRD diffractograms of 4 samples from the C1-Santaluz deposit. (A) Sample MP151-2 corresponds to a carbonaceous phyllite with white micas, chlorite and quartz; (B) Carbonaceous phyllite, which highlights graphite as well as microcline, chlorite and white micas; (C) Carbonaceous breccia composed of white micas, chlorite and quartz, and veins of quartz and albite; (D) Carbonaceous phyllite indicating the presence of muscovite, chlorite, quartz, and veins of quartz and albite.

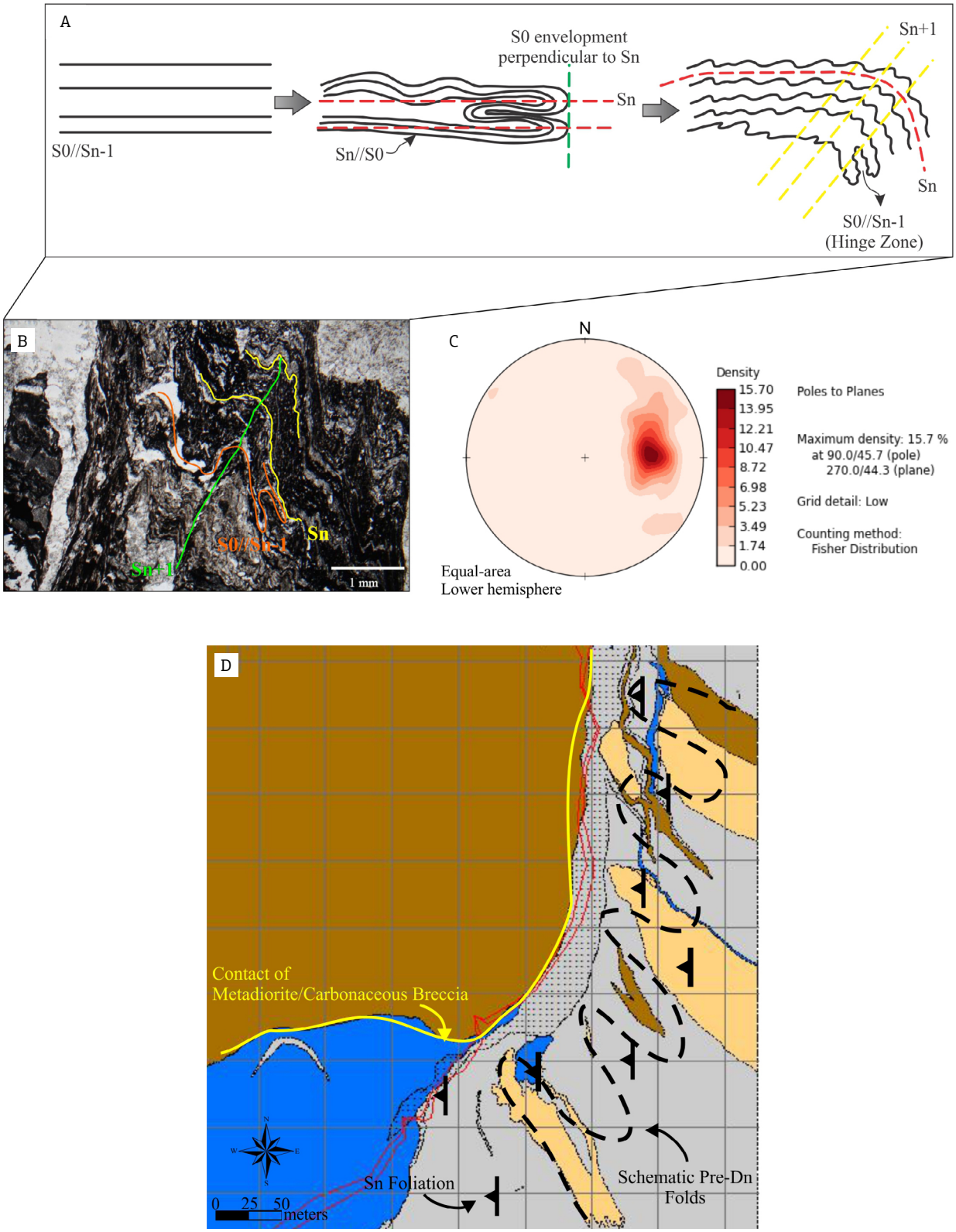

Figure 10. (A) Schematic illustration showing structures associated with the deformation phases in the studied area; (B) Cross-polarized, transmitted light photomicrograph of carbonaceous breccia thin section illustrating the main deformation features shown in A; (C) Stereogram of the D_{n-1} phase with the main $S_0//S_{n-1}$ direction (n = 83) observed mainly in chlorite-sericite-quartz schist, carbonaceous phyllite, and its contact with the metadiorite apophysis; (D) Part of the study area highlighting the pre-D_n folds that truncate the metadiorite/carbonaceous breccia contact (repeated layers of chlorite-sericite-quartz schist unit).

by a schistosity or crenulation cleavage (Fig. 11), depending on the rock type and the scale of observation.

In carbonaceous breccias, the S_0 compositional layering is parallel to the S_{n-1} foliation. Where folded (isoclinal folds), it forms the S_n schistosity (axial planar foliation). Moreover, quartz veins and veinlets are embedded in the compositional banding being deformed by the D_n deformation phase.

The S_n foliation has a N-S to NNW-SSE strike, dipping to the west and southwest, respectively. The attitude that reflects the general pattern of the study area is 266/50 (Fig. 11).

The intersection between S_n and the compositional banding S_0, parallel to the S_{n-1} foliation, has created an intersection lineation (L_{in}) on the S_n surface. This structure plunges to the NW (main attitude of 330/21, Fig. 11). The D_n folds

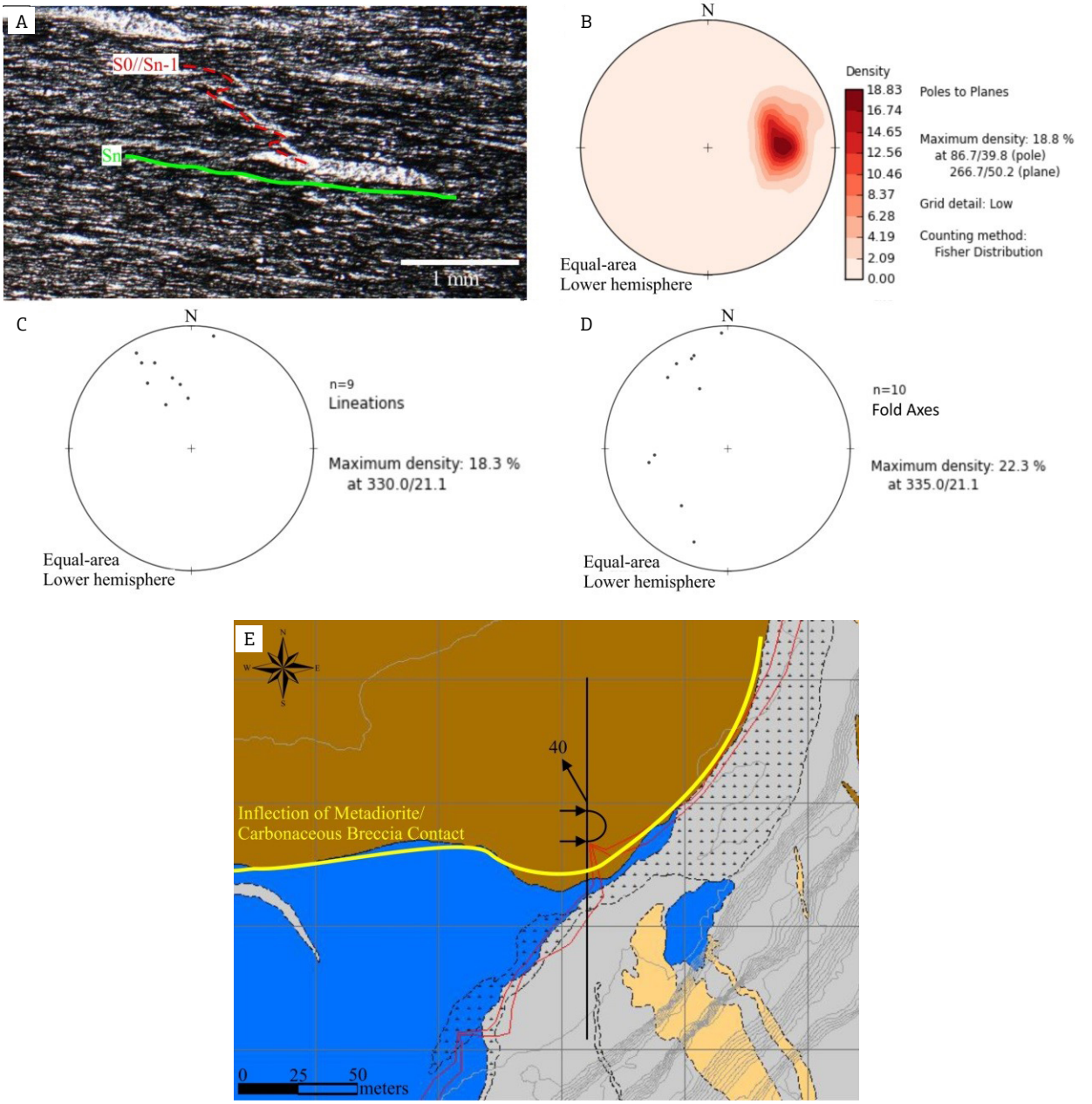

Figure 11. (A) Cross-polarized, transmitted light photomicrograph of thin section showing S_n foliation transposing $S_0//S_{n-1}$ in carbonaceous phyllite. (B) Stereogram of the S_n foliation (n = 127) of all lithotypes from the C1-Santaluz deposit. (C) Stereogram of intersection lineation of carbonaceous phyllite and chlorite-sericite-quartz schist. (D) Stereogram of D_n fold axes of the metasedimentary domain. (E) Inflection of the metadiorite/carbonaceous breccia contact marking of an overturned synform fold dipping to the northwest.

have an axis plunging to the NW (335/21, Fig. 11) and SW, subordinately. The intersection lineation is parallel-subparallel to the D_n fold axis.

The contact between the metadiorite and the carbonaceous breccia has a N-S strike in the northern part, but displays an E-W strike in the south-central area. This structure delineates an overturned synform (both flanks dipping to the NW) with an axis plunging to the NW (Fig. 11). While the contact (S_0) is oriented E-W, the S_n foliation is oriented N-S to NNW-SSE (the axial plane of this fold).

D_{n+1} Deformation Phase

The D_{n+1} phase is represented by folds and, locally, the crenulation cleavage S_{n+1}. The distribution of the structures associated with this deformation phase is not homogeneous throughout the area. The attitude of the S_{n+1} foliation varies along the area and only a few measurements could be made in the field. The S_{n+1} foliation has a NE-SW strike dipping to the NW and averaging 325/38 (Fig. 12). Also, the range of attitudes seems to indicate a subsequent deformational phase, in which the S_{n+1} foliation is folded. During D_{n+1}, sulfide minerals, mainly pyrite, appear to be embedded in the compositional banding S_0; where S_0 is folded, opaque minerals typically accompany this structure.

Metamorphism

The mineral assemblages in the C1-Santaluz rocks, with biotite, chlorite and muscovite, indicate a regional progressive metamorphism typical of the low greenschist facies, in the chlorite to the biotite zones (Fig. 13) (Barrow 1893; Tilley 1925). Although most of the chlorite is in equilibrium with biotite and muscovite, part of it may be product of later alteration. Actinolite was not identified in any of the studied rocks. The mineral assemblage described above, occurs in all studied lithotypes, as chlorite-sericite-quartz schist; carbonaceous phyllite; carbonaceous breccia, metandesite, metadacite and metadiorite.

Textures such as recrystallization of quartz grains in both metavolcanic and metasedimentary lithostratigraphic domains and saussuritization of plagioclase are also present. The recrystallization of the quartz crystals is displayed by subgrain rotation, which indicates lower temperature

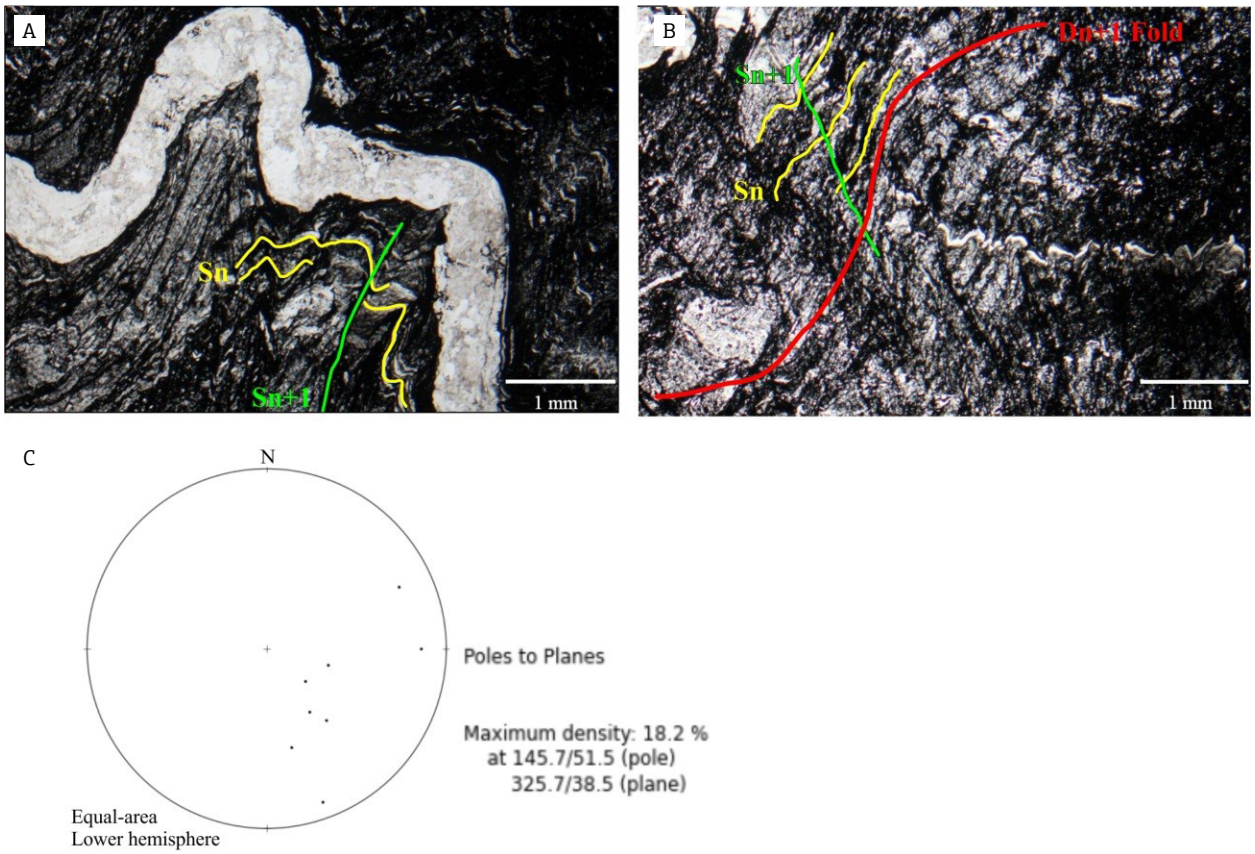

Figure 12. Cross-polarized, transmitted light photomicrographs of thin section showing: (A) An example of the S_{n+1} foliation (crenulation cleavage) of carbonaceous phyllite; (B) S_{n+1} crenulation cleavage highlighting to D_{n+1} fold in a carbonaceous phyllite; (C) Stereogram of S_{n+1} foliation in the metasedimentary domain.

environment, with a maximum temperature value of 400ºC (Eskola 1920, 1939, Miyashiro 1961, 1973, Turner 1981).

DISCUSSION

Lithological and mineralogical aspects

Geological mapping at the C1-Santaluz deposit reveals a complex stratigraphic sequence. It is difficult to separate the sub-units of the Rio Itapicuru greenstone belt because of the common alternation between lenses and apophyses of each domain into one another (*e.g.,* metavolcanic lenses present in the metasedimentary domain; chlorite-sericite-quartz schist layers inserted into the metavolcanic domain). This is why lithotypes are classified into domains. Moreover, the structural features of the deposit have an important role in the structural control of the gold mineralization (Figs. 10 and 11).

Gold mineralization is hosted in carbonaceous breccia, which is interpreted as a lithotectonic unit generated by the intrusion of the metadiorite body (metasubvolcanic intrusive) and/or metadacite unit (metavolcanic rocks domain; Fig. 5)

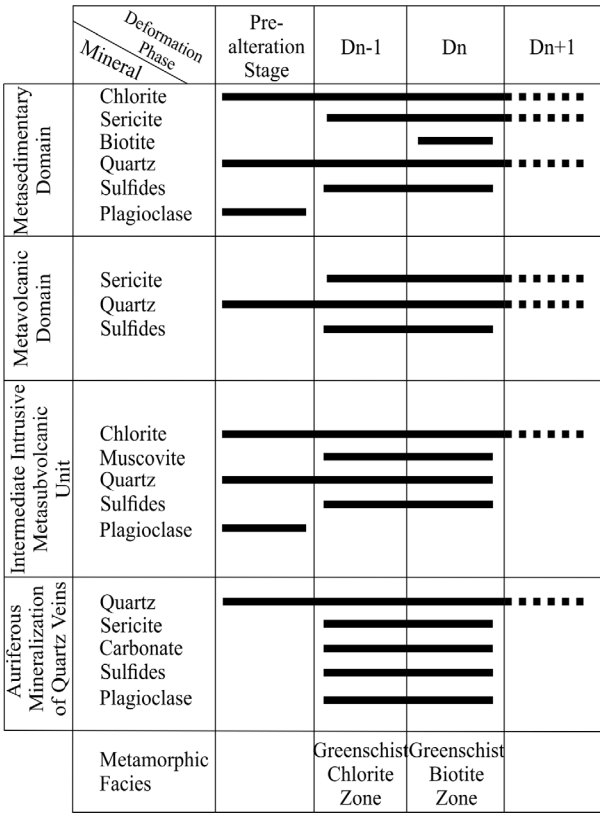

Figure 13. Mineralogical sequence according to the main lithotypes and deformational phases at the C1-Santaluz deposit.

in this carbonaceous rock. The contact of these two lithological domains is abrupt, and interpreted as a brittle/ductile shear zone, with a dip angle of 65º for both foliation S_n and the contact (S_0). Thus, the metadiorite may be used as a prospective guide, as it is easily recognizable in the field as well as in drill hole cores. This may be interpreted as a carbonaceous hydraulic breccia in light of the abundance of quartz veins and veinlets, which are commonly folded and ruptured. Besides, the top contact of the breccia with metadiorite is fractured.

In the C1-Santaluz deposit carbonaceous breccia hosts mineralized quartz veins, which are concordant (most commonly) or discordant to $S_n//S_0$, where the associated sulfide minerals are pyrite and arsenopyrite. The highest Au grades are typical of concordant veins (Yamana Gold Inc. data). Where carbonaceous breccia with veinlets host lenses of altered brecciated metadacite, gold results tend to increase (personal communication from Yamana Gold Inc. personnel). The presence of arsenopyrite, either in veins or in the host rock is indicative of mineralization. Gold deposition took place in the late stages of the ductile, shear event in which temperatures ranged from 360 to 420ºC (Xavier 1987).

SEM analyses show that pyrite replaces chalcopyrite, which often presents a cubic habit in subhedral-euhedral crystals. Pyrite also occurs as subhedral to euhedral crystals, as much in quartz veins as in the host rock. Though less common, sphalerite is identified as inclusions in chalcopyrite. Stibnite is present exclusively in quartz veins. In general, sulfide minerals cannot be directly used as guide to gold, although the presence of arsenopyrite in quartz veinlets or in the host rocks, associated or not with pyrite, suggests anomalous gold values.

The XRD data show the presence of graphite. With regards to metamorphic grade, a low temperature character is indicated by the low degree of crystallinity of graphite (Barrenechea *et al.* 1992, Suchy *et al.* 1997, Crespo *et al.* 2006). Graphite is only observed in one sample located in the contact region between the metadacite and carbonaceous breccia. Since this is a lithotectonic contact, it is possible that it provided enough heat to the system to favor its local development of this mineral phase. Furthermore, this contact may have aided the generation of arsenopyrite, which is typically deposited under low to moderate temperature in hydrothermal systems (lower or middle greenschist grades, Kretschmar & Scott 1976; 320 ± 30ºC, Kerrich & Hoder 1982). The presence of arsenopyrite is indicative of a low temperature formation correlating to the maximum metamorphic temperature of the C1-Santaluz deposit (400ºC), suggested by Xavier (1987) and the present contribution.

In the other three samples analyzed by XRD, carbonaceous material, and not graphite, is present. Additionally, carbonaceous

material occurs in quartz crystals interstices in the matrix, or even forming a surface layer on these same grains, suggesting that this material is not the only component of the carbonaceous phyllites or breccias.

Structural aspects and gold mineralization

The mineralized contact (metadiorite and carbonaceous breccia) is almost perpendicular to all other lithological units located in the eastern part of the deposit (Fig. 3). Furthermore, the study area has pre-D_n folds characterized by the repeating layers of the chlorite-sericite-quartz schist unit, and they are truncated by the metadiorite/carbonaceous breccias mineralized contact. All these features indicate that the metadiorite intrusion is syn-tectonic with respect to the shear zone marking this contact, and also represents a syn-D_n fault zone, since it has the same strike of the S_n foliation.

The D_n deformation phase corresponds to the main deformation phase of the area. It correlates with the D2 stage described by Chauvet *et al.* (1997), and is associated with the emplacement of the granitoid plutons in the RIGB, generating a N-S penetrative foliation in the rocks, also marked by shear zones with the same direction.

Mineralized quartz veins embedded in carbonaceous breccias appear associated with the S_n foliation, such as is the case in the northern and southern parts of the mine. However, in its central region, S_n maintains the same N-S to NNW-SSE direction and the lithological contacts show an E-W orientation. Thus, at this central portion, the mineralized bodies are lodged into the S_0 bedding. This suggests that the mineralized quartz veins in the study area may have been generated prior to the formation of the D_n phase, as they have already been constrained by $S_0//S_{n-1}$ structure, before deformation in the D_n phase (S_n schistosity).

Large *et al.* (2011) point out that in orogenic gold systems, the combination of both regional stratigraphic and local structural controls can define the host rock as well as possible ore shoots. Hinge zones of D_n folds may be able to concentrate and thicken gold mineralization. The intersection between a structure and a favorable lithotype can form geometric ore shoots (Squire *et al.* 2008). Thus, the relation between hinge zones of D_n folds and the carbonaceous breccia at the C1-Santaluz deposit represents a favorable loci for the formation of gold ore rods. The attitude of the intersection lineation between the S_0 compositional banding and S_n foliation (parallel to D_n fold axis) reinforces the importance of such conditions for mining purposes. This is particularly important in the C1-Santaluz as auriferous mineralization is associated with carbonaceous phyllite and breccia layers, where ore bodies are marked by quartz rods (D_n fold axis). These rods are thickening in the hinge zones of the D_n fold dipping to NW, where the compositional banding is perpendicular to the axial plane.

Peak metamorphic conditions were reached during the D_n phase, based on the presence of biotite formed and oriented according to the S_n foliation. Also, quartz in the matrix is typically granoblastic, deformed and/or stretched according to the preferred orientation of S_n. This feature suggests quartz recrystallization, and that subgrain rotation and recrystallization took place according to criteria of Passchier and Trouw (2006). In all rock domains, micaceous minerals define the S_n foliation and chlorite zones, and they characterize a lower greenschist facies assemblage. Biotite is observed to be an index mineral for the identified parageneses biotite-chlorite-sericite-quartz-albite, which is indicative of pressure and temperature values of approximately 4 kbar and 400ºC, respectively (Passchier & Trouw 2006).

As already presented before, part of the chlorite in the area is product of metamorphism, being in equilibrium with biotite and muscovite, and representing later alteration. Moreover, pre- and syn-alteration stages of the units may contain chlorite as a hydrothermal alteration product.

For the Fazenda Brasileiro deposit, Vieira *et al.* (1998) suggest that hydrothermal alteration is subdivided in five stages, of which four and five can be attributed to the formation of orebodies, and their mineral assemblages are represented mostly by chlorite, biotite, arsenopyrite, albite, carbonate and gold. An identical mineral assemblage related to the mineralized host rock has been observed by the present authors in the C1-Santaluz deposit.

CONCLUSIONS

The identified rocks of the studied area are represented by the metavolcanic and metasedimentary domains, and the intermediate intrusive metasubvolcanic lithotype. The schematic simplified lithotectonic column of the C1-Santaluz deposit proposed in this study is composed from base to the top by chlorite-sericite-quartz schist; carbonaceous phyllite; carbonaceous breccia (metasedimentary rocks domain); metandesite & metadacite (metavolcanic rocks domain); metadiorite (metamorphic intermediate intrusive rocks); and quartz veins and veinlets (auriferous mineralization of quartz veins). The metadiorite and the metadacite form abrupt contacts with the mineralized carbonaceous breccia. Therefore, the metasubvolcanic rock assists as a prospective guide for mining in this deposit, since the contact with the metasedimentary domain is easily recognized either in outcrops or in drill holes. This contact is interpreted as a lithotectonic contact, which acted as channels that favored the

flow of ore-bearing fluids, precipitating gold and related sulfides, such as arsenopyrite (Mihalasky 2001).

The SEM analyses show that gold is associated with arsenopyrite. The gold genesis is, therefore, directly related to the hydrothermal event that formed this sulfide mineral, either in quartz veins, carbonate-quartz veins, or in the rock matrix.

The XRD data show that most of the carbonaceous material is amorphous. Therefore, the term "carbonaceous material" is kept for the lithotypes carbonaceous phyllite and breccia.

In the C1-Santaluz deposit, three deformational phases are identified: D_{n-1}, D_n and D_{n+1}. Gold mineralization occurs in intrusive quartz veins and veinlets in carbonaceous breccia. These veins were probably formed during the D_{n-1} deformational phase, as they also occur in the compositional banding S_0. Mineralized veins, however, are also evident in hinge zones of D_n folds, with axis dipping to NW. Ore shoots appear to be controlled by the orientation of D_n fold axis, and as D_n transposed all previous structures, in regions far from D_n hinge zones, all planar structures and mineralized quartz veins are parallel. This explains why the quartz veins may occur parallel or discordant in respect to the compositional banding and the S_{n-1} foliation in the C1-Santaluz deposit.

ACKNOWLEDGEMENTS

The authors wish to thank Yamana Gold Inc. for their assistance during field work and also supporting data analysis. We also thank reviewers of the Brazilian Journal of Geology for helping improve the manuscript.

REFERENCES

Alkmim F.F. 2004. O que faz de um Cráton um Cráton? O Cráton do São Francisco e as Revelações Almeidianas a Delimitá-lo. *In*: Mantesso-Neto V. (Ed.). *Geologia do Continente Sul-Americano:* Evolução da Obra de Fernando Flávio Marques de Almeida. São Paulo, Beca, p. 18-35.

Almeida F.F.M. 1977. O Cráton do São Francisco. *Revista Brasileira de Geociências*, **7**:349-364.

Almeida F.F.M. Hasui Y., Brito Neves B.B. 1976. The upper precambrian of South America. *Boletim do Instituto de Geociências*, Universidade de São Paulo, **7**:45-80.

Almeida F.F.M., Hasui Y., Brito Neves B.B., Fuck R.A. 1981. Brazilian Structural Provinces: an introduction. *Earth Sciences Reviews*, **17**:1-29. https://doi.org/10.1016/0012-8252(81)90003-9

Alves da Silva F.C. 1994. *Etude Structural du Greenstone Belt Paleoproterozoique du Rio Itapicuru (Bahia, Brésil).* PhD Thesis, Université d'Orleans, Orleans, França, 307 p.

Alves da Silva F.C., Chauvet A., Faure M. 1998. General features of the gold deposits in the Rio Itapicuru greenstone belt (RIGB, NE Brazil): discussion of the origin, timing and tectonic model. *Revista Brasileira de Geociências*, **28**(3):377-390.

Assis J.A.C. 2016. *Geologia do Depósito de Ouro de C1-Santaluz no Greenstone Belt do Rio Itapicuru, Brasil*. MS Dissertation, Instituto de Geociências e Ciências Exatas, Universidade Estadual Paulista "Júlio de Mesquita Filho", Rio Claro, 123 p.

Barbosa J.S.F., Sabaté P. 2002. Geological features and the Paleoproterozoic collision of four Archean crustal segments of the São Francisco Cráton, Bahia, Brazil. A synthesis. *Anais da Academia Brasileira de Ciências*, **74**:343-359. http://doi.org/10.1590/S0001-37652002000200009

Barbosa J.S.F., Sabaté P. 2004. Archean and Paleoproterozoic Crust of São Francisco Craton, Bahia, Brazil: Geodynamic Features. *Precambrian Research*, **133**:1-27. http://doi.org/10.1016/j.precamres.2004.03.001

Barrenechea J.F., Rodas M., Arche A. 1992. Relation between graphitization of organic matter and clay mineralogy, Silurian black shales in Central Spain. *Mineralogical Magazine*, **56**:477-485. https://doi.org/10.1180/minmag.1992.056.385.04

Barrow G. 1893. On an Intrusion of Muscovite-biotite Gneiss in the South-eastern Highlands of Scotland, and its accompanying Metamorphism. *Quarterly Journal of the Geological Society of London*, **49**:330-358. https://doi.org/10.1144/GSL.JGS.1893.049.01-04.52

Brio Gold Inc. Available from: <http://briogoldinc.com/operations/santa-luz/>. Accessed on: May 7, 2017.

Carvalho E.D.R. 1991. *Caracterização petrográfica e geoquímica das litologias na Mina de Ouro Fazenda Maria Preta no Greenstone Belt do Rio Itapicuru, Bahia.* MS Dissertation, Instituto de Geociências, Universidade Estadual de Campinas, Campinas, 88 p.

Carvalho M.J., Oliveira E.P. 2003. Geologia do Tonalito Itareru, bloco Serrinha, Bahia: uma intrusão sin-tectônica do início da colisão continental no segmento norte do Orógeno Itabuna Salvador-Curaçá. *Revista Brasileirade Geociências*, **33**:55-68.

Chauvet A., Alves da Silva F.C., Faure M., Guerrot C. 1997. Structural evolution of the Paleoproterozoic Rio Itapicuru granite-greenstone belt (Bahia, Brazil): the role of syn kinematic plutons in the regional tectonics. *Precambrian Research*, **84**:139-162.

Coelho C.E.S., Silva F.H.F. 1998. The structural control of the gold deposits of the Fazenda Maria Preta gold district at Rio Itapicuru Greenstone Belt, northeastern Brazil. *Revista Brasileira de Geociências*, **28**(3):367-376.

Colvine A.C., Andrews A.J., Cherry M.E., Durocher M.E., Fyon J.A., Lavigne M.J., MacDonald A.J., Marmont S. 1984. *An integrated model for the origin of Archean lode gold deposits*. Ontário: Ontario Geological Survey, 98 p.

Crespo E., Luque F.J., Barrenechea J.F, Rodas M. 2006. Influence of grinding on graphite crystallinity from experimental and natural data: implications for graphite thermometry and sample preparation. *Mineralogical Magazine*, **70**(6):697-707. https://doi.org/10.1180/0026461067060358

Cruz Filho B.E., Conceição H., Rosa M.L.S., Rios D.C., Macambira M.J.B., Marinho M.M. 2005. Geocronologia e assinatura isotópica (Rb-Sr e Sm-Nd) do batólito trondhjemítico Nordestina, Núcleo Serrinha, Nordeste do Estado da Bahia. *Revista Brasileira de Geociências*, **35**(4 Supl.):1e8.

Donatti Filho J.P. 2007. *Reavaliação do Contexto Tectônico dos Basaltos do Greenstone Belt do Rio Itapicuru (Bahia), com base na Geoquímica de Elementos-Traço*. MS Dissertation, Instituto de Geociências, Universidade Estadual de Campinas, Campinas, 62 p.

Donatti Filho J.P., Oliveira E.P., McNaughton N.J. 2013. Provenance of zircon xenocrysts in the Neoproterozoic Brauna Kimberlite Field, São Francisco Craton, Brazil: Evidence for a thick Paleoproterozoic lithosphere beneath the Serrinha block. *Journal of South American Earth Science*, **45**:83-96. http://ib.adnxs.com/seg?add=1&redir=http%3A%2F%2Fdx.doi.org%2F10.1016%2Fj.jsames.2013.03.001

Donatti Filho J.P., Tappe S., Elson P., Oliveira E.P., Heaman L. 2012. Age and origin of the Neoproterozoic Brauna kimberlites: melt generation within the metasomatized base of the São Francisco craton, Brazil. *Chemical Geology*, **353**:19-35. https://doi.org/2010.1016/j.chemgeo.2012.06.004

Eskola P. 1920. The mineral facies of rocks. *Norsk Geologisk Tidsskrift*, **6**:143-194.

Eskola P. 1939. Die metamorphen Gesteine. *In*: Barth T.F.W., Correns C.W., Eskola P. (eds.), *Die Entstehung der Gesteine*. Berlin, Springer, p. 422.

Gaál G., Teixeira J.B.G., D'el Rey Silva L.J.H., Silva M.G. 1987. New U-Pb data from granitoids, reflecting Early Proterozoic crustal evolution in northeast Bahia, Brazil. *In*: International Symposium on Granites and Associated Mineralizations. Salvador, Bahia, Brazil: SBG (unpublished).

Goldfarb R.J., Baker T., Dubé B., Groves D.I., Hart C.J.R., Gosselin P. 2005. Distribution, character, and genesis of gold deposits in metamorphic terran. *Economic Geology 100th Anniversary*, 407-450.

Goldfabr R.J., Groves D.I. 2015. Orogenic gold: Common or evolving fluid and metal sources through time. *Lithos*, **233**:2-26.

Goldfarb R.J., Groves D.I., Gardoll S. 2001. Orogenic gold and geologic time: a global synthesis. *Ore Geology Reviews*, **18**:1-75. https://doi.org/10.1016/S0169-1368(01)00016-6

Grisólia M.F.P. 2010. *Proveniência de rochas metassedimentares do Greenstone Belt do Rio Itapicuru, Bahia*. MS Dissertation, Instituto de Geociências, Universidade Estadual de Campinas, Campinas, 108 p.

Groves D.I., Goldfarb R.J., Gebre-Mariam M., Hagemann S.G., Robert F. 1998. Orogenis gold deposits: A proposed classification in the context of their crustal distribution and relationship to other gold deposit types. *Ore Geology Reviews*, **13**:7-27.

Groves D.I., Goldfarb R.J., Knox-Robinson C.M., Ojala J., Gardoll S., Yun G.Y, Holyland P. 2000. Late-kinematic timing of orogenic gold deposits and significance for computer-based exploration techniques with emphasis on the Yilgarn Block, Western Australia. *Ore Geology Reviews*, **17**:1-38.

Groves D.I., Goldfarb R.J., Robert F., Hart C.J.R. 2003. Gold deposits in metamorphic belts: overview of current understanding, outstanding problems, future research, and exploration significance. *Economic Geology*, **98**(1):1-29. https://doi.org/10.2113/gsecongeo.98.1.1

Hagemann S.G., Cassidy K.F. 2000. Archean orogenic lode gold deposits. *In*: Hagemann S.G., Brown P.E. (eds.), Gold in 2000. *Reviews in Economic Geology*, **13**:9-68.

Kerrich R., Hoder R.W. 1982. Archean lode gold and base metal deposits; chemical evidence for metal separation into independent hydrothermal systems. *Canadian Institute of Mining and Metallurgy*, **24**:144-160.

Kishida A. 1979. *Caracterização geológica e geoquímica das sequências vulcanossedimentares do médio Rio Itapicuru (Bahia)*. MS Dissertation, Universidade Federal da Bahia, Salvador, 98 p.

Kishida A., Riccio L. 1980. Chemostratigraphy of lava sequences from the Rio Itapicuru Greenstone Belt, Bahia, Brazil. *Precambrian Research*, **11**:161-178. http://dx.doi.org/10.1016/0301-9268(80)90044-3

Kretschmar U., Scott S.D. 1976. Phase relations involving arsenopyrite in the system Fe-As-S and their application. *Canadian Mineralogist*, **14**:364-386.

Large R.R., Bull S.W., Maslennikov V.V. 2011. A carbonaceous sedimentary source-rock model for carlin-type and orogenic gold deposits. *Economic Geology and The Bulletin of The Society of Economic Geologists*, **106**(3):331-358.

Marimom M.P.C, Kishida A., Teixeira J.B.G. 1986. Estudo da alteração hidrotermal relacionada à mineralização aurífera da Fazenda Brasileiro - BA. *In*: Congresso Brasileiro de Geologia, 34., Goiânia. *Anais...*, v. 4, p. 1556-1570.

Marinho M.M. 1991. *La Séquence Volcano-Sedimentaire de Contendas–Mirante et la Bordure Occidentale du Bloc Jequié (Cráton du São Francisco-Brésil): Un exemple de Transition Archéean-Protérozoique*. PhD Thesis, Blaise Pascal University, Clermont Ferrand, França, 388 p.

Mello E.F., Assis C.M., Orlandi P.H., Costa H.C., Albuquerque R., Silva G.L.P., Xavier R.P. 1996. Contribuição à tipologia dos veios auríferos da Mina Fazenda Brasileiro, greenstone belt do Rio Itapicuru, BA. *In*: Congresso Brasileiro de Geologia, 38., Camboriú. *Anais*, v. 3, p. 238-241.

Mello E.F., Xavier R.P., McNaughton N.J., Hagemann S.G., Fletcher I., Snee L. 2006. Age constraints on felsic intrusions, metamorphism and gold mineralization in the Paleoproterozoic Rio Itapicuru greenstone belt, NE Bahia State, Brazil. *Mineralium Deposita*, **40**:849-866. http://ib.adnxs.com/seg?add=1&redir=http%3A%2F%2Fdx.doi.org%2F10.1007%2Fs00126-005-0037-3

Mihalasky M.J. 2001. *Mineral potential modelling of gold and silver mineralisation in the Nevada Great Basin: a GIS-based analysis using weights of evidence*. USGS Open-File Report, 448 p. https://doi.org/10.3133/ofr01291

Miyashiro A. 1961. Evolution of metamorphic belts. *Journal of Petrology*, **2**:277-311. https://doi.org/10.1093/petrology/2.3.277

Miyashiro A. 1973. *Metamorphism and metamorphic belts*. London, Allen & Unwin, 492 p.

Oliveira E.P., Lafon J.M., Souza Z.S. 1998. A Paleoproterozoic age for the Rio Capim volcano-plutonic sequence, Bahia, Brazil: whole-rock Pb-Pb, Pb-evaporation and U-Pb constraints. *In*: Congresso Brasileiro de Geologia, 15., Belo Horizonte. *Anais*, p. 14.

Oliveira E.P., McNaughton N.J., Armstrong R. 2010. Mesoarchaean to Palaeoproterozoic growth of the northern segment of the Itabuna-Salvador-Curaçá Orogen, São Francisco Craton, Brazil. Special Publication. *In*: Kusky T.M., Zhai M.-G., Xiao W. (eds.), *The Evolving Continents:* Understanding Processes of Continental Growth. London, Geological Society of London, 338, p. 263-286.

Passchier C.W., Trouw R.A.J. 2006. *Microtectonics*. New York, Springer-Verlag, 366 p.

Pimentel M.M., Silva M.G. 2003. Sm-Nd age of the Fazenda Brasileiro gabbro, Bahia, Brazil: Example of robust behavior of the Sm-Nd isotopic system under extreme hydrothermal alteration. *Anais da Academia Brasileira de Ciências*, **75**(3):383-392. http://dx.doi.org/10.1590/S0001-37652003000300009

Reinhardt M.C. 1988. *Controles lito-estruturais da mineralização aurífera em zona de cisalhamento da Mina Fazenda Brasileiro, Bahia*. MS Dissertation, Instituto de Geociências, Universidade Federal da Bahia, Salvador.

Reinhardt M.C., Davison I. 1989. Controle litoestrutural dos corpos auríferos da mina Fazenda Brasileiro, Bahia, Brasil. *Revista Brasileira de Geociências*, **19**(2):121-131.

Rios D.C., Conceição H., Davis D.W., Rosa M.L.S., Macambira M.J.B., Dickin A.P. 2003. A New Proposal for the Subdivision of Granitic Rocks at Serrinha Nucleus, Bahia, Brazil, Based on U-Pb and Pb-Pb Geochronological and Lithogeochemical Data. *In*: South American Symposium on Isotope Geology, Salvador. *Short Papers*, p. 264.

Rios D.C., Conceição H., Davis D.W., Rosa M.L.S., Marinho M.M. 2005. Expansão do magmatismo granítico pós-orogênico no núcleo Serrinha (NE Bahia), cráton do São Francisco: idade U-Pb do maciço granítico Pedra Vermelha. *Revista Brasileira de Geociências*, **35**:423-426.

Rios D.C., Davis D.W., Conceição H., Macambira M.J.B., Peixoto A.A., Cruz Filho B.E., Oliveira L.L. 2000. Ages of granites of the Serrinha Nucleus, Bahia (Brazil): an overview. *Revista Brasileira de Geociências*, **30**:74-77.

Robert F. 1996. Quartz–carbonate vein gold. *In*: Eckstrand O.R., Sinclair W.D., Thorpe R.I. (eds.), *Geology of Canadian Mineral Deposit Types*. The Geology of North America. Boulder, Geological Society of America, p. 350-366.

Rocha Neto M.B. 1994. *Geologia e recursos minerais do Greenstone Belt do Rio Itapicuru, Bahia*. Série Arquivos Abertos. Bahia, Companhia Baiana de Pesquisa Mineral, **4**, 30 p.

Ruggiero A. 2008. *A unidade Maria Preta: geologia, geoquímica e petrogênese de rochas vulcânicas e sub-vulcânicas intermediárias a félsicas no "Greenstone Belt" do Rio Itapicuru, Bahia*. MS Dissertation, Instituto de Geociências, Universidade Estadual de Campinas, Campinas, 62 p.

Silva M.G. 1983. *A seqüência vulcanossedimentar do médio Rio Itapicuru, Bahia: caracterização petrográfica, considerações petrogenéticas preliminares e zoneografia metamórfica*. MS Dissertation, Instituto de Geociências, Universidade Federal da Bahia, Salvador, 88 p.

Silva M.G. 1992. O Greenstone Belt do Rio Itapicuru: Uma bacia do tipo back-arc fóssil. *Revista Brasileira de Geociências*, **22**(2):157-166.

Silva M.G., Coelho C.E.S., Teixeira J.B.G., Alves da Silva F.C., Silva R.A., Souza J.A.B. 2001. The Rio Itapicuru greenstone belt, Bahia, Brazil: geologic evolution and review of gold mineralization. *Mineralium Deposita*, **36**:345-357. https://doi.org/10.1007/s001260100173

Squire R.J., Robinson J.A., Rawling T.J., Wilson C.J.L. 2008. Controls on Ore Shoot Locations and Geometries at the Stawell Gold Mine, Southeastern Australia: Contributions of the Volcanosedimentary, Alteration, and Structural Architecture. *Economic Geology*, **103**:1029-1041. https://doi.org/10.2113/gsecongeo.103.5.1029

Suchy V., Frey M., Wolf M. 1997. Vitrinite reflectance and shear-induced graphitization in orogenic belts: A case study from Kandersteg area, Helvetic Alps, Switzerland. *International Journal of Coal Geology*, **34**:1-20. https://doi.org/10.1016/S0166-5162(97)00018-9

Teixeira J.B.G. 1984. *Geologia e controles da mineralização aurífera em Fazenda Brasileiro, Serrinha (BA)*. MS Dissertation, Instituto de Geociências, Universidade Federal da Bahia, Salvador, 88 p.

Teixeira J.B.G., Kishida A., Marimon M.P.C., Xavier R.P., McReath I. 1990. The Fazenda Brasileiro gold deposit, Bahia; geology, hydrothermal alteration, and fluid inclusion studies. *Economic Geology*, **85**(5):990-1009. https://doi.org/10.2113/gsecongeo.85.5.990

Tilley C.E. 1925. Metamorphic Zones in the Southern Highlands of Scotland. *Quarterly Journal of the Geological Society*, **81**:100-112.

Turner F.J. 1981. *Metamorphic Petrology*. 2ª ed. New York, McGraw-Hill, 524 p.

Vasconcelos P., Becker, T. 1992. A idade da mineralização aurífera no depósito da Fazenda Brasileiro, Bahia, Brasil. *In*: Workshop em Metalogênese: Pesquisas atuais e novas tendências. Campinas, Universidade Estadual de Campinas. *Boletim de Resumos*, Campinas, p. 29.

Vieira M.B.H., Lobato L.M., Assis C.M., Gomes F.C.A., Silva R.A., Nascimento O.S., Orlandi P.H. 1998. Contribuição ao estudo da alteração hidrotermal na Mina de Ouro de Fazenda Brasileiro, Bahia. *In*: Congresso Brasileiro de Geologia, 40., Belo Horizonte, p. 130-130.

Xavier R.P. 1987. *Estudos de inclusões fluidas na mina de ouro da Fazenda Brasileiro, Greenstone Belt do Rio Itapicuru, Bahia*. MS Dissertation, Instituto de Geociências, Universidade de São Paulo, São Paulo, 142 p.